AD-A100 649 MASSACHUSETTS INST OF TECH CAMBRIDGE DEPT OF ELECTRI--ETC F/G 7/4
MICRODIELECTROMETRY.(U)
JUN 81 S D SENTURIA, N F SHEPPARD N00014-78-C-0591

UNCLASSIFIED NL

1 OF 1
AD-
A100649

END
DATE
FILMED
7-81
DTIC

LEVEL

AD A100649

OFFICE OF NAVAL RESEARCH

Contract N00014-78-C-0591

Task No. NR 356-691

TECHNICAL REPORT NO. 3

MICRODIELECTROMETRY

by

Stephen D. Senturia, Norman F. Sheppard, Steven L. Garverick,
Huan L. Lee and David R. Day

Paper presented at

A Critical Review:
Techniques for the Characterization of
Composite Materials

June 1981
Cambridge, MA

DTIC ELECTE JUN 26 1981 C

MASSACHUSETTS INSTITUTE OF TECHNOLOGY
Department of Electrical Engineering and Computer Science
and Center for Materials Science and Engineering
Cambridge, Massachusetts

June 8, 1981

Reproduction in whole or in part is permitted for any
purpose of the United States Government.

This document has been approved for public release and
sale; its distribution is unlimited.

DTIC FILE COPY

81 6 26 055

UNCLASSIFIED

SECURITY CLASSIFICATION OF THIS PAGE (When Data Entered)

REPORT DOCUMENTATION PAGE		READ INSTRUCTIONS BEFORE COMPLETING FORM
1. REPORT NUMBER	2. GOVT ACCESSION NO. AD-A100 649	3. RECIPIENT'S CATALOG NUMBER
4. TITLE (and Subtitle) Microdielectrometry		5. TYPE OF REPORT & PERIOD COVERED Technical Report 4/80-6/81
		6. PERFORMING ORG. REPORT NUMBER Technical Report No. 3
7. AUTHOR(s) Stephen D. Senturia, Norman F. Sheppard, Steven L. Garverick, Huan L. Lee, David R. DAy		8. CONTRACT OR GRANT NUMBER(s) N00014-78-C-0591, NSF-DMR 78-247
9. PERFORMING ORGANIZATION NAME AND ADDRESS Massachusetts Institute of Technology Department of Electrical Engineering and Computer Science, Cambridge, Ma 02139		10. PROGRAM ELEMENT, PROJECT, TASK AREA & WORK UNIT NUMBERS NR 356-691
11. CONTROLLING OFFICE NAME AND ADDRESS Department of the Navy, Office of Naval Research 800 N. Quincy Street, Arlington VA 22217 Code 427		12. REPORT DATE June 8, 1981
		13. NUMBER OF PAGES 22
14. MONITORING AGENCY NAME & ADDRESS (if different from Controlling Office) Technical rept. Apr 80-Jun 81		15. SECURITY CLASS. (of this report) UNCLASSIFIED
		15a. DECLASSIFICATION/DOWNGRADING SCHEDULE

16. DISTRIBUTION STATEMENT (of this Report)

This document has been approved for public release and sale; its distribution is unlimited.

17. DISTRIBUTION STATEMENT (of the abstract entered in Block 20, if different from Report)

18. SUPPLEMENTARY NOTES

19. KEY WORDS (Continue on reverse side if necessary and identify by block number)

Dielectrometry, cure monitoring, epoxy, integrated circuit, charge-flow transistor

20. ABSTRACT (Continue on reverse side if necessary and identify by block number)

Microdielectrometry, a new cure monitoring method, is used to monitor the cure of DGEBA/MDPA at three different temperatures. The basic device and measurement system, its calibration, and data interpretation are explained. The data are shown to yield a dielectric relaxation time that can be correlated with the variation of resin viscosity during cure prior to gelation.

DD FORM 1 JAN 73 1473 EDITION OF 1 NOV 65 IS OBSOLETE S/N 0102-LF-014-6601

UNCLASSIFIED 409490

SECURITY CLASSIFICATION OF THIS PAGE (When Data Entered)

MICRODIELECTROMETRY

Stephen D. Senturia, Norman F. Sheppard, Steven L. Garverick,
Huan L. Lee, and David R. Day

Department of Electrical Engineering and Computer Science, and
Center for Materials Science and Engineering
Massachusetts Institute of Technology
Cambridge MA 02139

ABSTRACT

The low-frequency dielectric properties of resins provide a useful tool for characterization both of the curing process and of fully cured material. We have used integrated circuit technology to develop a miniaturized dielectric probe that combines small size with built-in amplification to achieve sensitivity at frequencies as low as 1 Hz. The device combines a planar interdigitated electrode structure with a pair of matched field-effect transistors. The microdielectrometer "chip" can be implanted in a specimen, or a small sample of material (a few milligrams) can be placed on the active area of the device. When combined with an off-chip electronic feedback system, the device can be used to measure the complex dielectric constant of the sample material either as it cures, or after cure. The device is capable of operating at temperatures up to 200°C, making it useful for a wide variety of curing and post-cure studies. Device calibration is based on a two dimensional computer model which has been experimentally confirmed for a variety of control samples. Several typical applications are illustrated by experiments, and the use of the data to follow changes in the dominant low-frequency dielectric relaxation during the cure of a model epoxy resin system are presented.

A

I. INTRODUCTION

This paper presents a new microelectronic technique for the measurement of low-frequency dielectric properties of materials, with particular emphasis on application to the in-situ monitoring of resin cure (1). Measurements of dielectric properties of polymers and other materials are used in a variety of applications (2). In the case of resin cure, the technique has proved sufficiently useful to prompt the development of commercial instrumentation dedicated to this application (3). This commercial "dielectrometer" instrument uses a conventional parallel plate capacitor geometry, either in fixed plate form or in the form of thin foils to which leads can be attached, and operates in the nominal frequency range 100 Hz to 100 kHz.

The technique that we call "microdielectrometry" differs from the conventional measurement in several ways. First, it uses as sense electrodes a pair of very small planar interdigitated electrodes fabricated as part of a silicon integrated circuit (the "microdielectrometer" chip). This electrode geometry, while much less efficient than the parallel plate geometry in terms of electric field coupling between the electrodes, can be manufactured with great precision using microelectronic techniques, and therefore can yield an electrode pattern with known and highly reproducible calibration. Second, the technique incorporates high impedance amplifiers in the form of depletion-mode MOSFET's built into the microdielectrometer chip, achieving a sensitivity improvement that more than compensates for the relatively inefficient electrode structure, and permits succesful operation of the device down to 1 Hz and below, an advantage for studying slow relaxations in materials. Finally, with the use of a specially designed electronic feedback circuit, such potential sources of problems as FET temperature and pressure dependences can be cancelled out, permitting the microdielectrometer chip to be used over a wide temperature range (up to 250°C), even when implanted in a bulk specimen of curing material.

Section II of this paper contains a description of the microdielectrometer device and accompanying measurement system. Section III presents examples of the raw data, in the form of gain-phase plots, obtained during the cure of a two-component epoxy-amine system (DGEBA/MPDA). Section IV illustrates how this raw data can be converted into the conventional real and imaginary parts of the dielectric constant by the use of calibration curves developed from two-dimensional computer simulations of the device. Finally, Section V demonstrates how the resulting dielectric constant data can be interpreted to obtain a dynamical relaxation time which is shown to be strongly correlated with the behavior of the viscosity during cure.

II. THE MICRODIELECTROMETER CHIP AND MEASUREMENT SYSTEM

The microdielectrometer chip contains a planar interdigitated electrode and two depletion-mode metal-oxide-semiconductor field-effect transistors (MOSFET's). A top view of a portion of the device is shown in Fig. 1. The outer electrode is called the driven gate, and is connected to a normal bonding pad. The inner electrode is called the floating gate, and extends

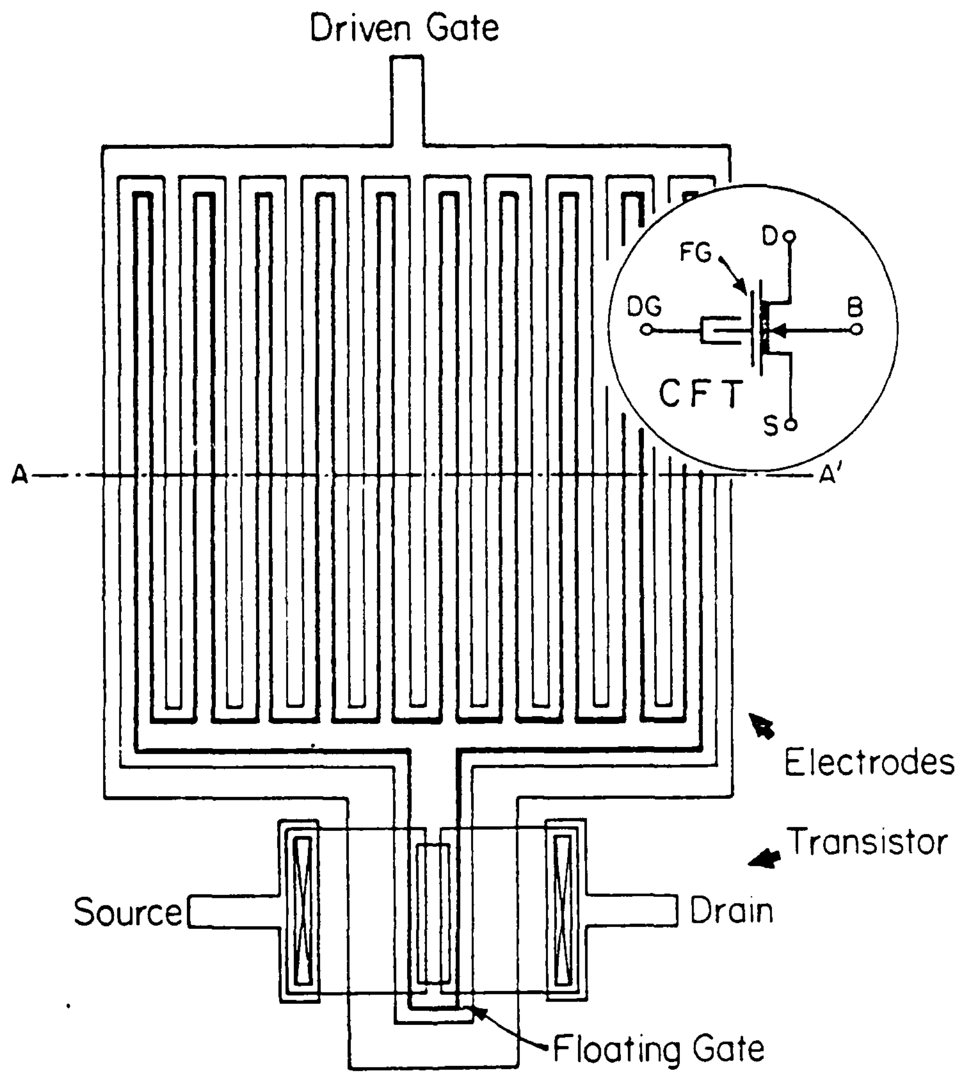

Fig. 1 Top view of sensor portion of microdielectrometer chip

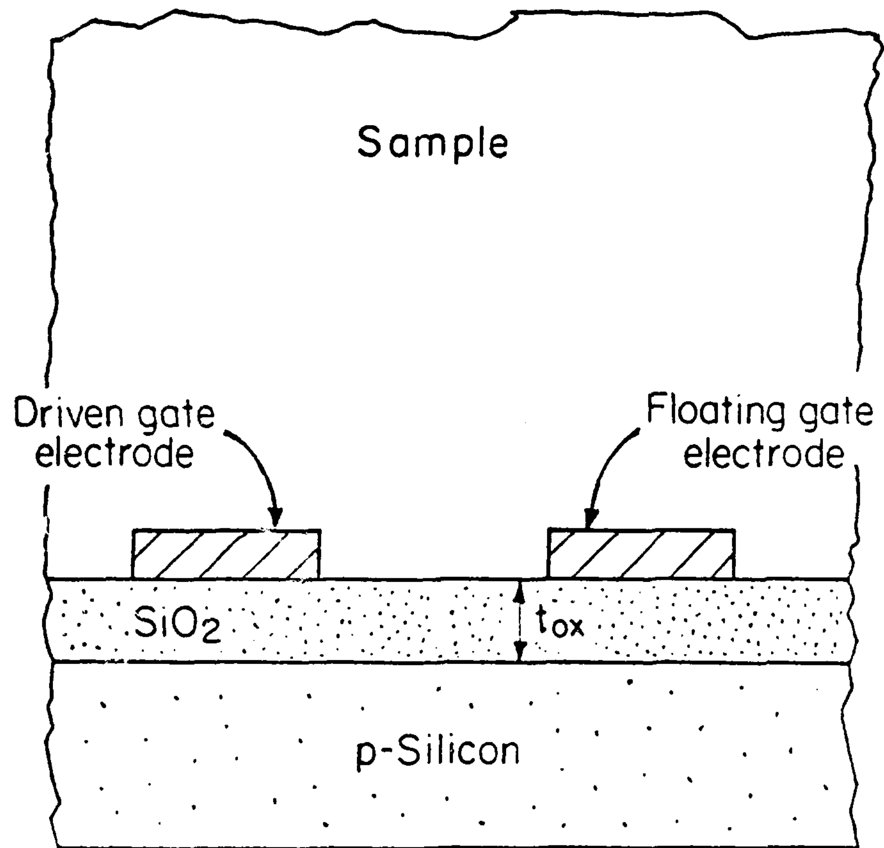

Fig. 2 Cross section of electrode portion of microdielectrometer

over the channel region of one of the FET's as shown. The silicon dioxide layer between the floating gate and the silicon substrate effectively isolates the floating gate, with the result that there is no electrical connection between the driven and floating gate except through the sample material under study, which is placed over the electrodes as in the schematic cross section in Fig. 2. A sinusoidal voltage applied to the driven gate causes time-varying current (both conduction and displacement current) to flow through the sample toward the floating gate. The capacitance between the floating gate and the substrate collects the charge from this current, this time-varying charge on the floating gate serving to modulate the conductance of the FET channel. Thus, the primary measurement consists of determining the magnitude and phase of the charge on the floating gate produced by a sinusoidal waveform applied to the driven gate. Clearly, this will depend on the dielectric properties of the sample.

In order that the measurement not depend on the electrical characteristics of the FET's (which are subject to manufacture-related variations as well as temperature and pressure dependences), two identical FET's are fabricated on the microdielectrometer chip. The second "reference" FET is connected in a specially designed feedback "interface circuit" which permits measurement of the floating gate voltage by applying to the gate of the reference FET exactly that voltage required to make the two FET currents identical. The details of this circuit are described elsewhere (4).

The microdielectrometer chip as presently designed is 75 mils square, and has a total of eight contacts. The device is mounted onto a standard TO-8 transistor header, and wire bonded. Other, more compact mounting and packaging methods could also be used. The device can be used either by placing a small sample of material over the electrodes or by implanting the entire device into a bulk specimen. In either case, the device can readily be placed in an oven for isothermal or ramped temperature studies. Because of the feedback circuit, no temperature compensation of the measurement is required.

A block diagram of the instrumentation system is shown in Fig. 3. The device and interface circuit are connected to a computer-controlled function generator, and the magnitude and phase of the floating gate voltage are measured with a gain-phase meter, also linked to the computer. As will be explained in more detail below, the transfer function between the driven gate and the floating gate depends only on the real and imaginary parts of the dielectric constant (ε' and ε''), and not explicitly on the frequency of the sinusoid. Therefore, there is a unique mapping between measured gain and phase, on the one hand, and ε' and ε'' on the other hand. At present, the graphics display on the HP-85 computer used to run the system is set up for real-time display of the gain-phase characteristic. Typical data for a cure cycle will be presented in the following section. Other components of the system include a link to a larger computer (HP-1000), and access to line printers, cassette storage, and a graphics plotter. All data is stored in files on cassette, permitting very flexible data analysis procedures and with no transcription or re-formatting required.

Fig. 3

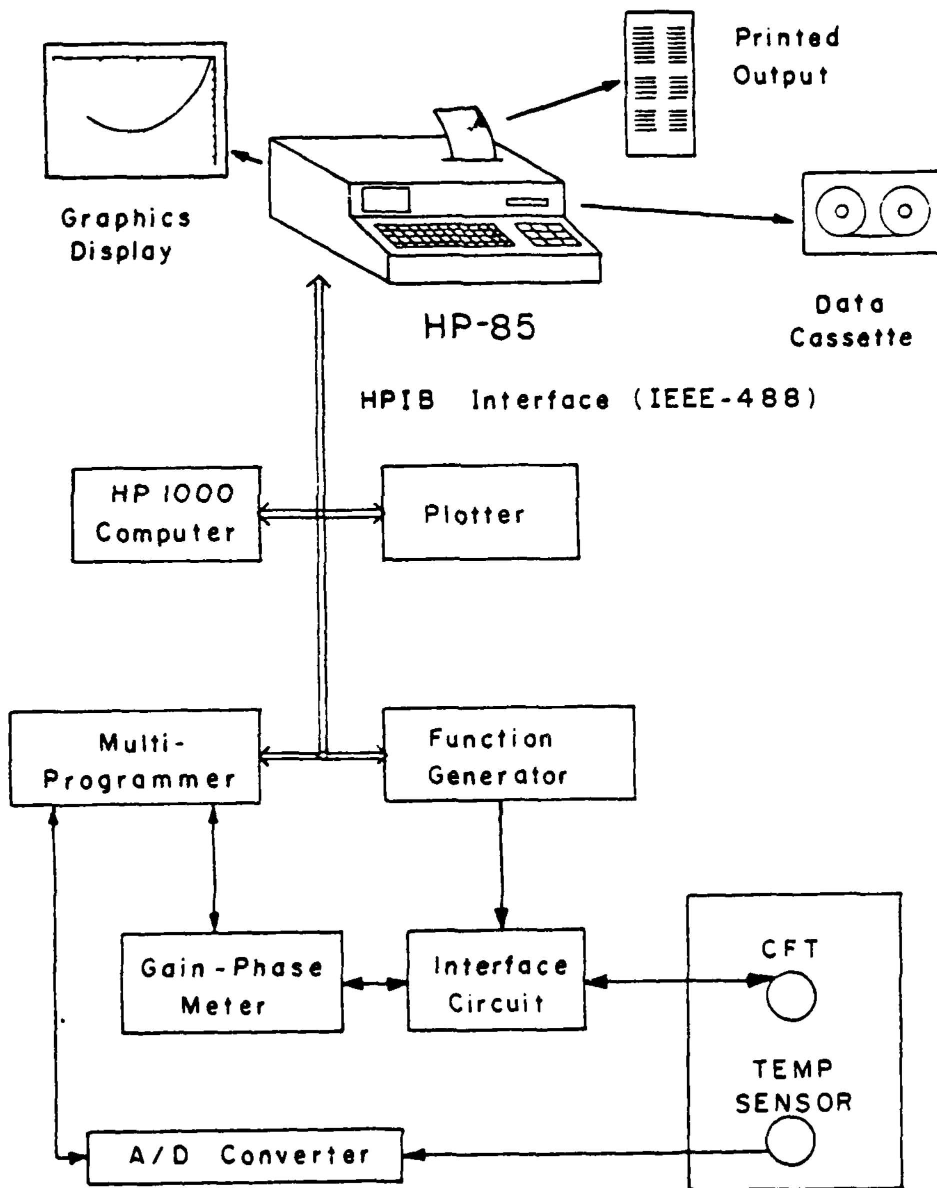

III. GAIN-PHASE DATA

The typical experimental sequence is established by a program residing in the HP-85. The operator selects a set of frequencies to be used, and establishes how often measurements are desired. Following initiation of a run, the computer automatically sequences the frequency of the function generator, waits a prescribed settling time, and then records the magnitude and phase of the floating gate voltage from the gain-phase meter.

Figure 4 illustrates a typical run as seen from the graphics display of the HP-85. The sample consists of a stoichimetric mix of DGEBA and MPDA, cured at 80°C, on a device with an oxide thickness of 10,000 Å. For each measurement, a point is plotted in gain-phase space. In the first photograph, two sets of readings at each of seven frequencies have been completed. The pair of points farthest from the origin correspond to 1000 Hz, the next pair to 300 Hz. The remaining points are still clustered at the origin, an expected result given the relatively high conductance of the resin early in cure.

The second photograph shows the display ten minutes later. Two more measurement sequences have been completed. One can easily visualize the "trajectories" followed by the data for each frequency in gain-phase space as the resin cures. As will be explained in Section IV, the trajectory for a particular frequency is due to the variation of the dielectric properties (at that frequency) during cure.

This particular resin system shows a remarkably simple behavior of the various trajectories: they all overlap. The data for 300 Hz follow the same path through gain-phase space as the data for 1000 Hz. Indeed, throughout the frequency range 1-1000 Hz, the data follow a single trajectory with only minor variations, as shown in the third photograph in Fig. 4, taken at the end of cure. Two major trajectories are seen, a primary large trajectory, and a second small trajectory late in cure. The only important difference between the data for the different frequencies is how fast the point moves around the path of the trajectory. The highest frequency goes first, and the lowest frequency last. The strong structure inherent in the data suggests that the behavior of this resin can be modeled with simple relaxation times. This subject is discussed further in Section V.

That the cure trajectory is a well behaved property of the resin system is illustrated by a comparison of the plots in Fig. 5. Figs. 5a and 5b show data from cures at two different temperatures. The path followed is virtually identical in the two cases, but because of the lower temperature, the 60°C data requires a longer time to move across the gain-phase trajectory.

The importance of the device dimensions is illustrated by a comparison of Figs. 5b and 5c. The data in each case are for a cure at 100 C, but the device in Fig. 5c has a thinner oxide layer, resulting in a different apparent gain-phase trajectory. However, since the device dimensions are different, one would expect that the mapping between gain-phase and ε', ε'' might differ. Indeed, it will be shown below that the dielectric data obtained from these two devices using the appropriate calibration curves are the same.

Fig. 4

TYPICAL CURE DATA

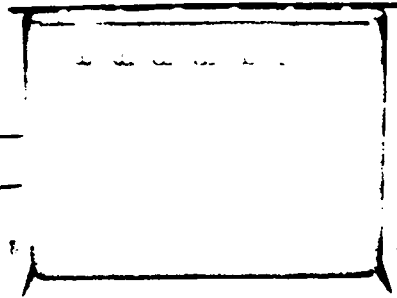

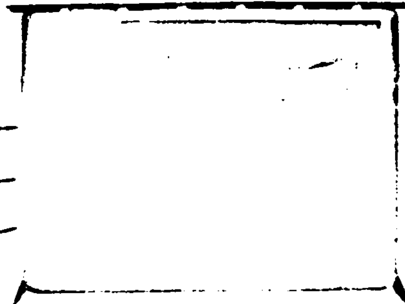

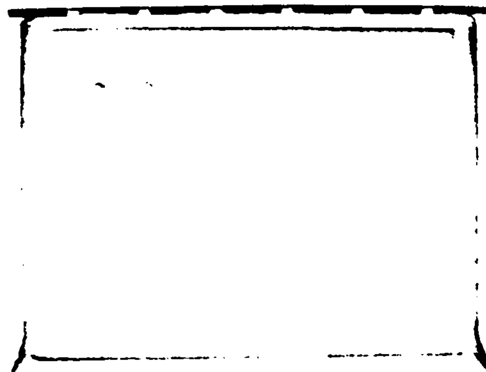

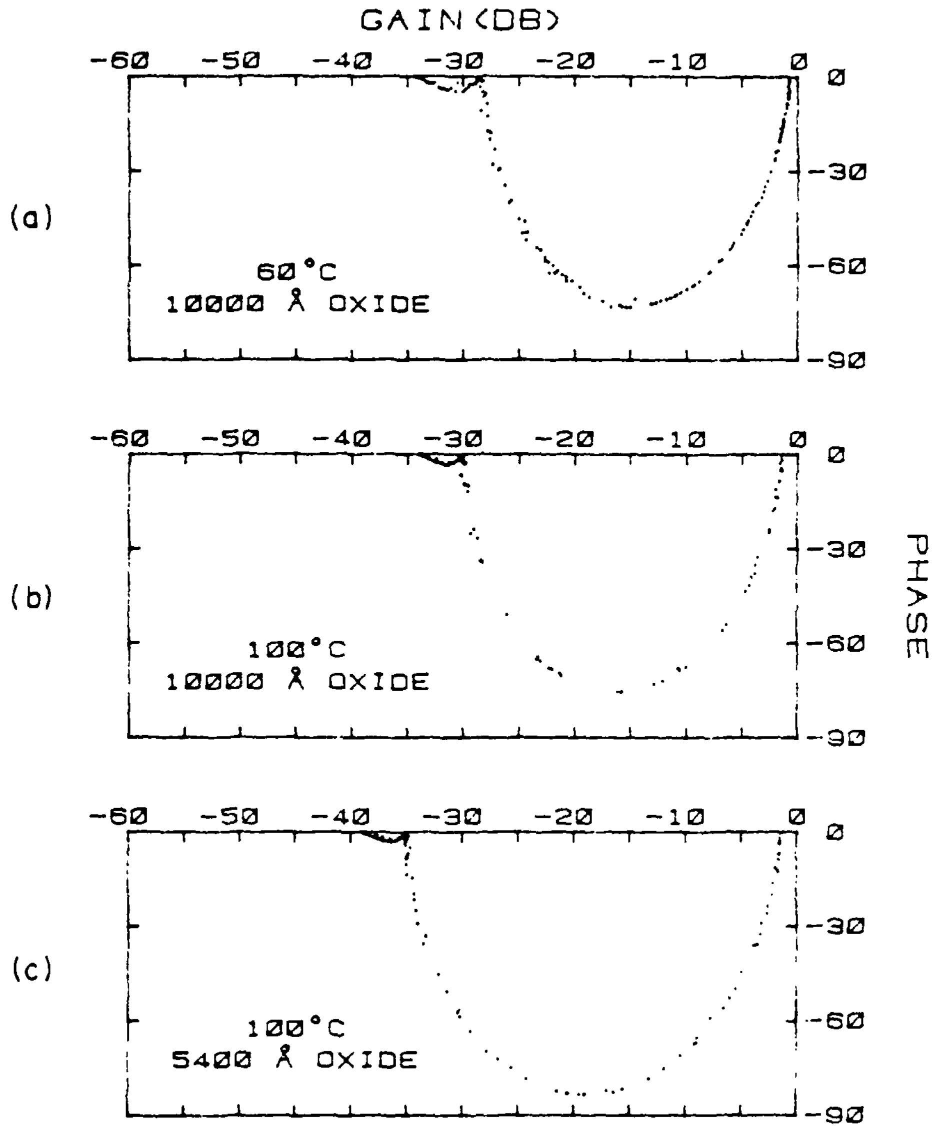

Fig. 5 Gain-phase data for DGEBA/MPDA a) 60°C cure, 10000 Å oxide, b) 100°C cure, 10000 Å oxide, c) 100°C cure, 5400 Å oxide

It is important to note that the present system configuration, in which the raw data is displayed in gain-phase format, can be replaced by a display in which ε' and ε'' are the primary variables. This modification is planned for the near future.

IV. EXTRACTION OF DIELECTRIC DATA FROM GAIN-PHASE DATA

There is a unique correspondance or mapping between the gain-phase data and the real and imaginary parts of the sample dielectric constant (ε' and ε''). Calibration of the microdielectrometer device consists of determining this mapping. The first device models were based on a very approximate distributed RC transmission line (1). This paper uses a much more accurate calibration procedure in which a two-dimensional numerical solution to Laplace's equation is obtained using a complex amplitude for the potential, thereby permitting the effects of both the dielectric constant ε' and the dielectric loss ε'' to be included on an equal footing. This is important since early in the cure, the conductance, or loss term can dominate, whereas toward the end of cure, the dielectric term always dominates. Details of the calibration calculation are available elsewhere (5).

Figure 6 shows a typical set of calibration curves obtained for the device with the 10,000 Å oxide. Several features can be noted. For a perfect dielectric ($\varepsilon'' = 0$), the gain-phase points lie on the gain axis (zero phase shift). This permits a check of the calculated calibration by measuring the high-frequency transfer function of the device in air ($\varepsilon' = 1.0$). The accuracy of the in-air calibration is found to be better than 1 dB for both oxide thicknesses used in these experiments. Examination of the calibration curves shows that near the origin (corresponding to early in cure), the various curves crowd together. This means that the measurement is most prone to error when the data are near the origin, and that small gain offsets or spurious sources of either magnitude or phase errors might produce problems early in cure. Indeed, we have had problems with the calibration for gains above -3 dB, due to a spurious conduction path in the chip design which creates magnitude and phase errors when the resin is highly conductive, and due to a small gain offset (of order 1 dB) between the floating gate FET and reference FET. The details of the origins of these errors, their implications for the interpretation of measurements early in cure, and ways to remove the errors in future designs will be discussed elsewhere (6). For the present discussion, we have elected to ignore all data closer to the origin than -3 dB, and have compensated for the gain offset by a small correction for each device which makes the final high-frequency dielectric constant agree with the result of a parallel plate capacitor measurement on fully cured material. In no case is the gain correction more than 1.2 dB.

The time dependence of ε' and ε'' at three different frequencies for each of the runs illustrated in Figs. 5a, 5b, and 5c are plotted in Figs. 7, 8, and 9. Times to gelation t_g for this resin system are also shown for reference (7). Figs. 8 and 9, which correspond to different device geometries but the same cure temperature, show excellent agreement with one another. This demonstrates that the calibration procedure is basically correct. Comparison between Figs. 7 and 8, corresponding to the same device geometry but differ-

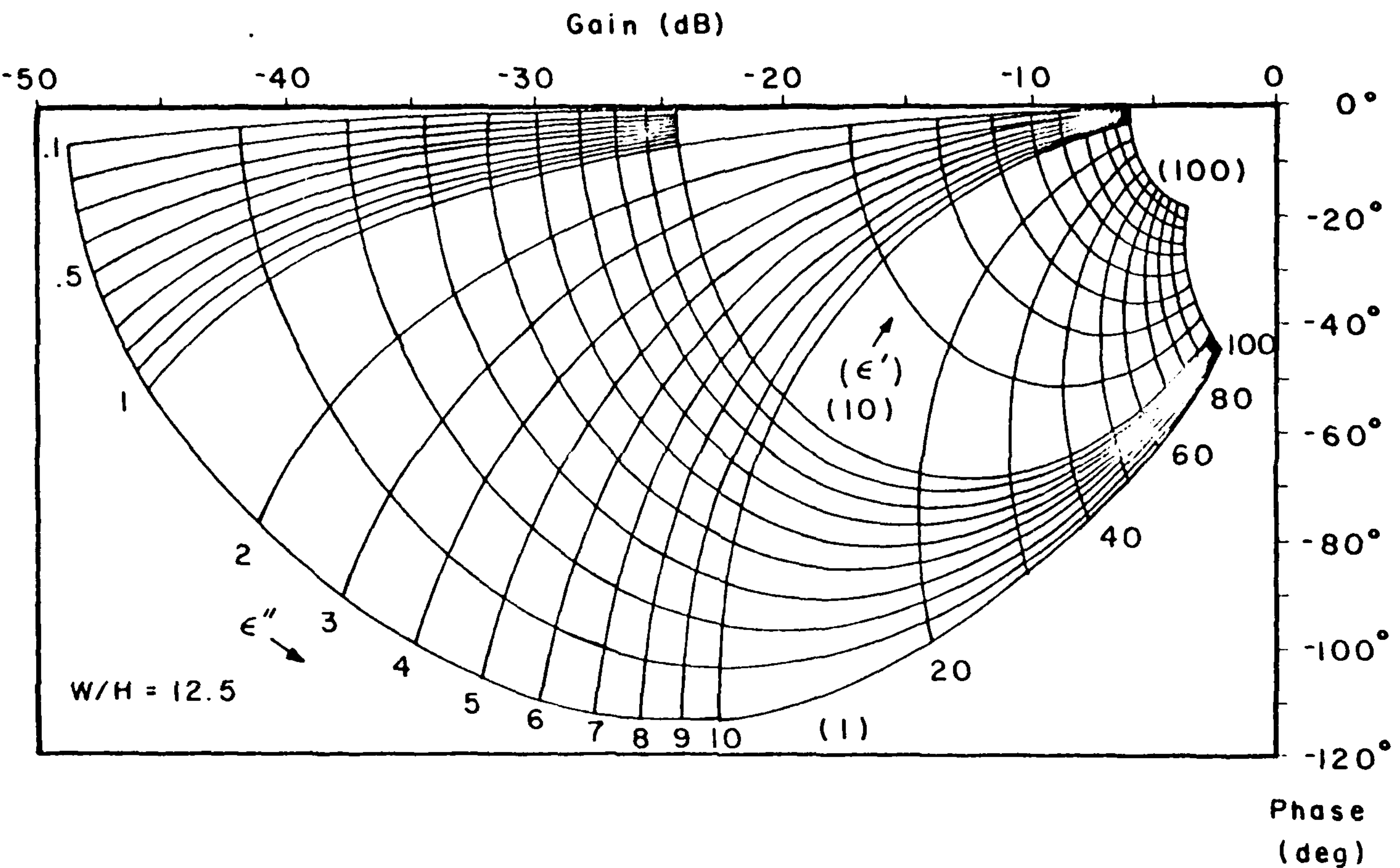

Fig. 6 Calibration plot showing contours of constant permittivity (ε') and loss factor (ε")

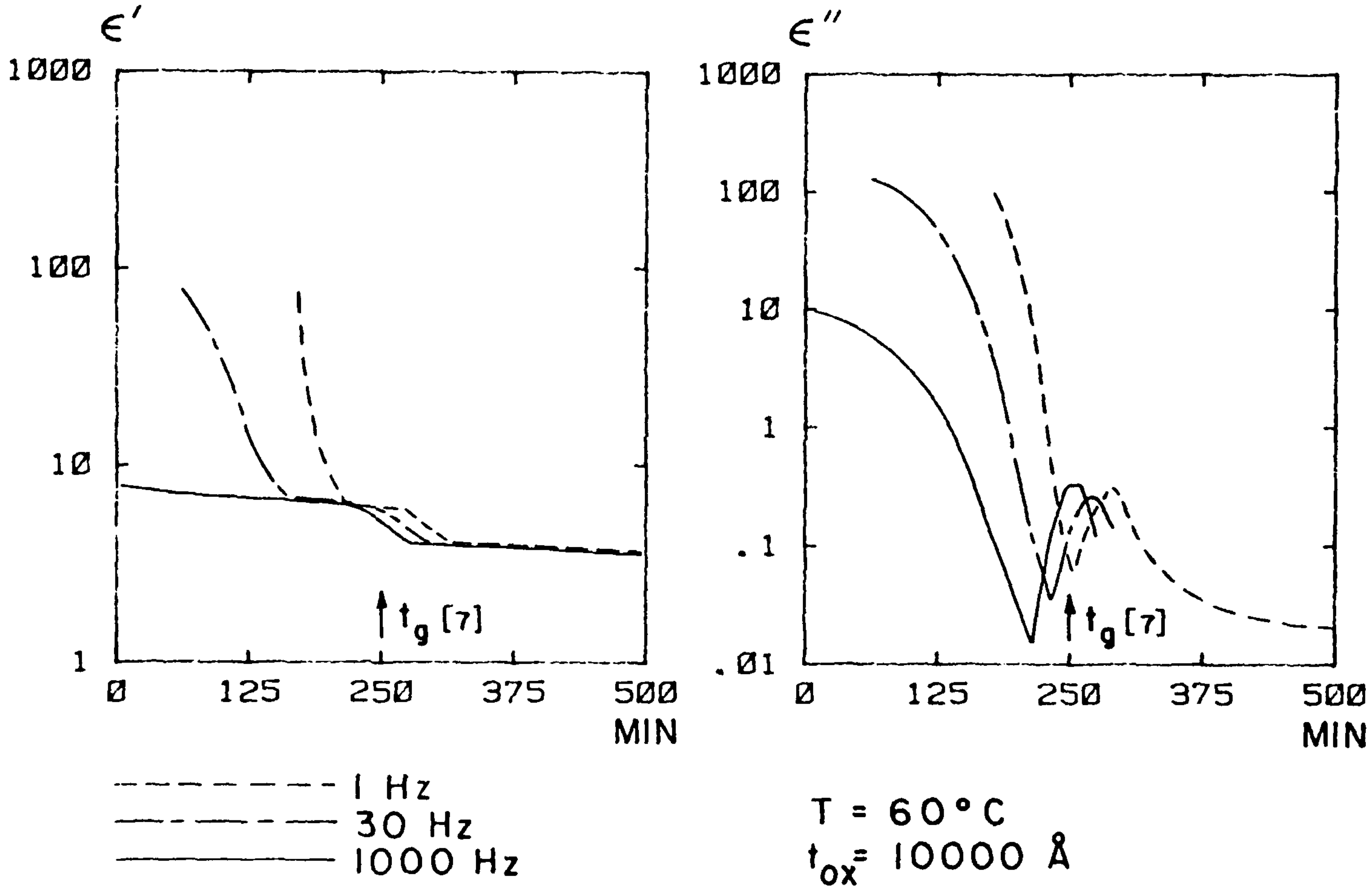

Fig. 7 Time dependence of ε' and ε" for data of Fig. 5a

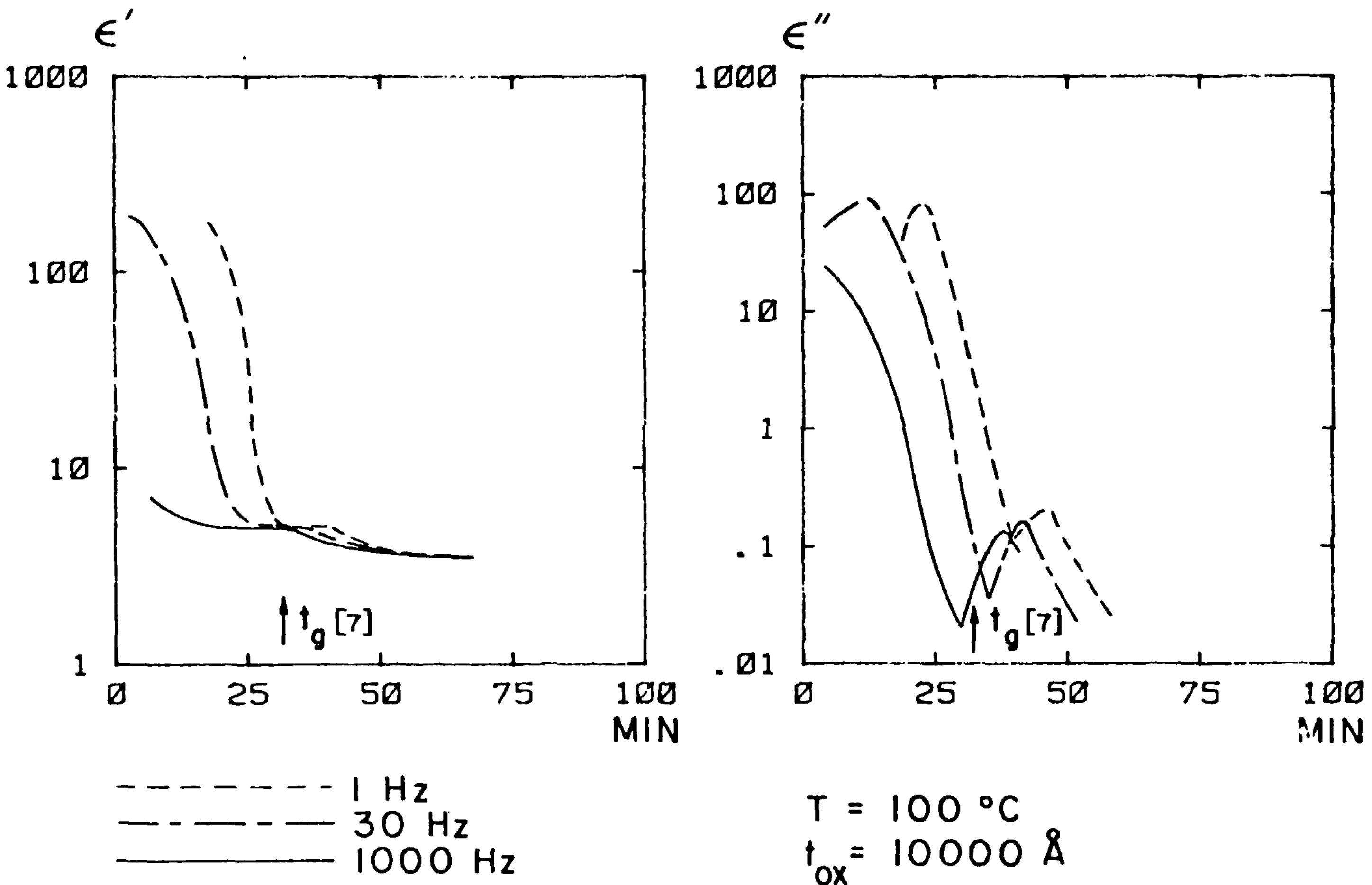

Fig. 8 Time dependence of ε' and ε" for data of Fig. 5b

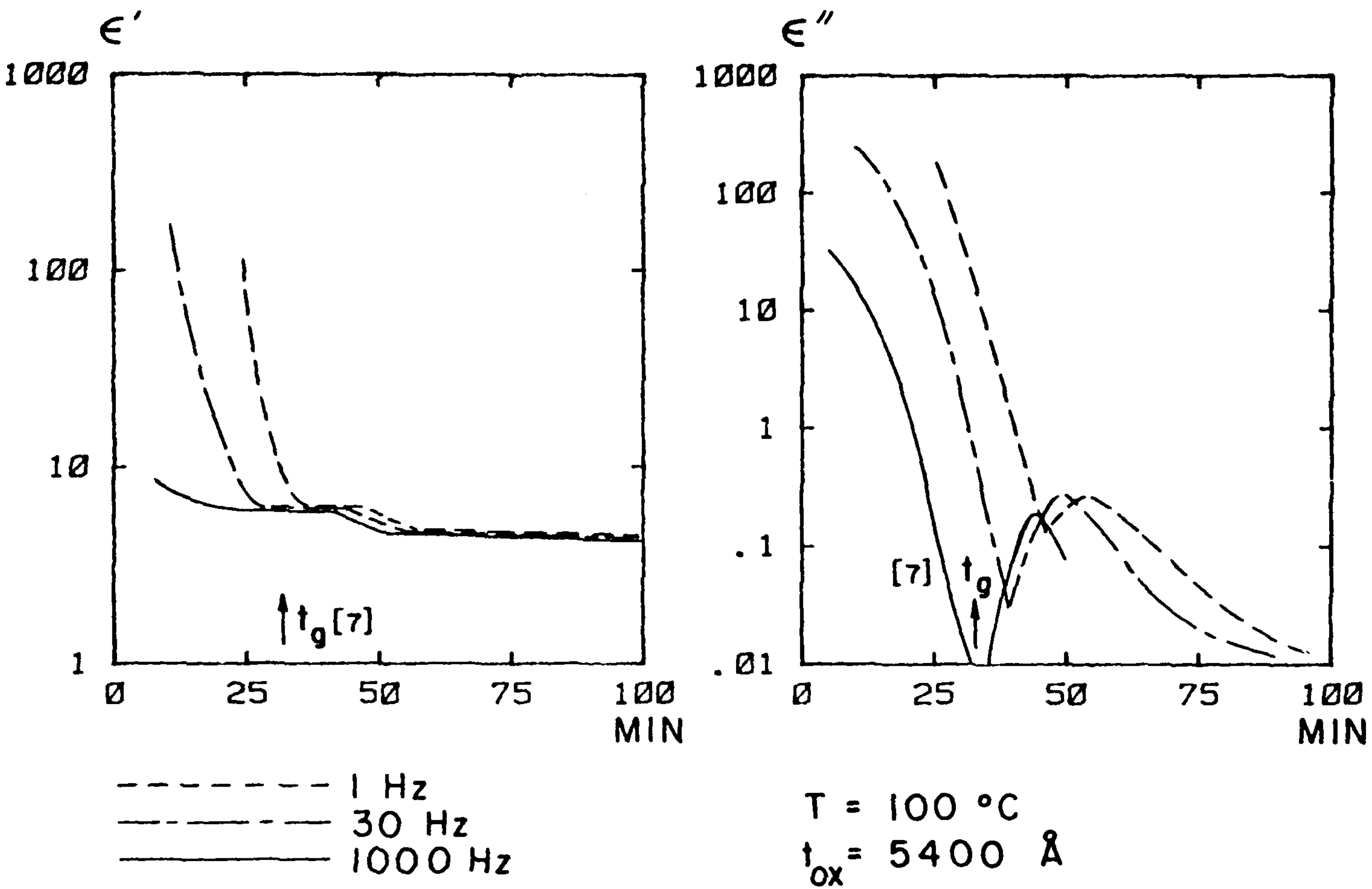

Fig. 9 Time dependence of ε' and ε" for data of Fig 5c

ent cure temperatures, shows that the changing features of the dielectric constant are the same, but occur over a longer time scale as the temperature is decreased, due to the activation of the curing reaction.

The results in Figs. 7 and 8 show that two relaxations are occuring: a large one prior to gelation, and a smaller one after gelation. The frequency dependence demonstrates that the 1 Hz measurement is more sensitive to these relaxations than higher frequencies, which is consistent with a model of dipole orientation. Increased frequency or extent of cure makes it more difficult for the dipoles to respond to the alternating electric field. This leads us to attribute the first relaxation to the increasing viscosity of the liquid phase as the epoxy polymerizes and approaches gelation, and the second to further crosslinking in the gel phase. The principal conclusion is that reliable low frequency dielectric data can be obtained with this device, and with the improved low-frequency sensitivity, direct comparison with other measurement techniques, such as torsional braid analysis, becomes possible.

V. INTERPRETATION WITH A RELAXATION TIME MODEL

The dielectric data presented in the previous section show a great deal of structure. In particular, prior to the classical gelation time, there is a strong dielectric relaxation evident. It can be easily shown that if the dielectric properties of a material obey a simple Debye model (that is, a model for the dielectric constant in which the frequency dependence is described by a single relaxation time), and if only the relaxation time changes with cure conditions, then one would expect all the trajectories in gain-phase space to overlap, as they do in our experiments. This prompted us to attempt to fit the data with a relaxation time model, and to determine how this relaxation time varies with cure.

A good way to examine relaxation time models is to plot ε'' versus ε' (the so-called Cole-Cole plot (8)), using frequency as the plotting parameter. If the Debye model holds, the data lie on a semicircle. The position of a point on the semicircle is determined by the product of the angular frequency and the relaxation time, so knowledge of the frequency permits determination of the relaxation time.

Fig. 10 shows a Cole-Cole plot for the data of Fig. 8 prior to gelation. The points correspond to the values of ε' and ε'', and the dashed curve represents the case for an ideal Debye model having a limiting low frequency dielectric constant of 450 and a limiting high frequency dielectric constant of 6. Agreement with the Debye model is seen to be very good. It should be emphasized that although it appears that only a small portion of the semicircle is covered by the data, the fit to the ideal Debye model is justified by the fact that the approach of the data to the ε' axis is fully perpendicular (8).

The relaxation time was determined at each point in cure prior to gelation, and the results are plotted in Fig. 11 for each of the six devices tested (two oxide thicknesses at each of three temperatures). For any one device, the agreement between the relaxation times determined from different

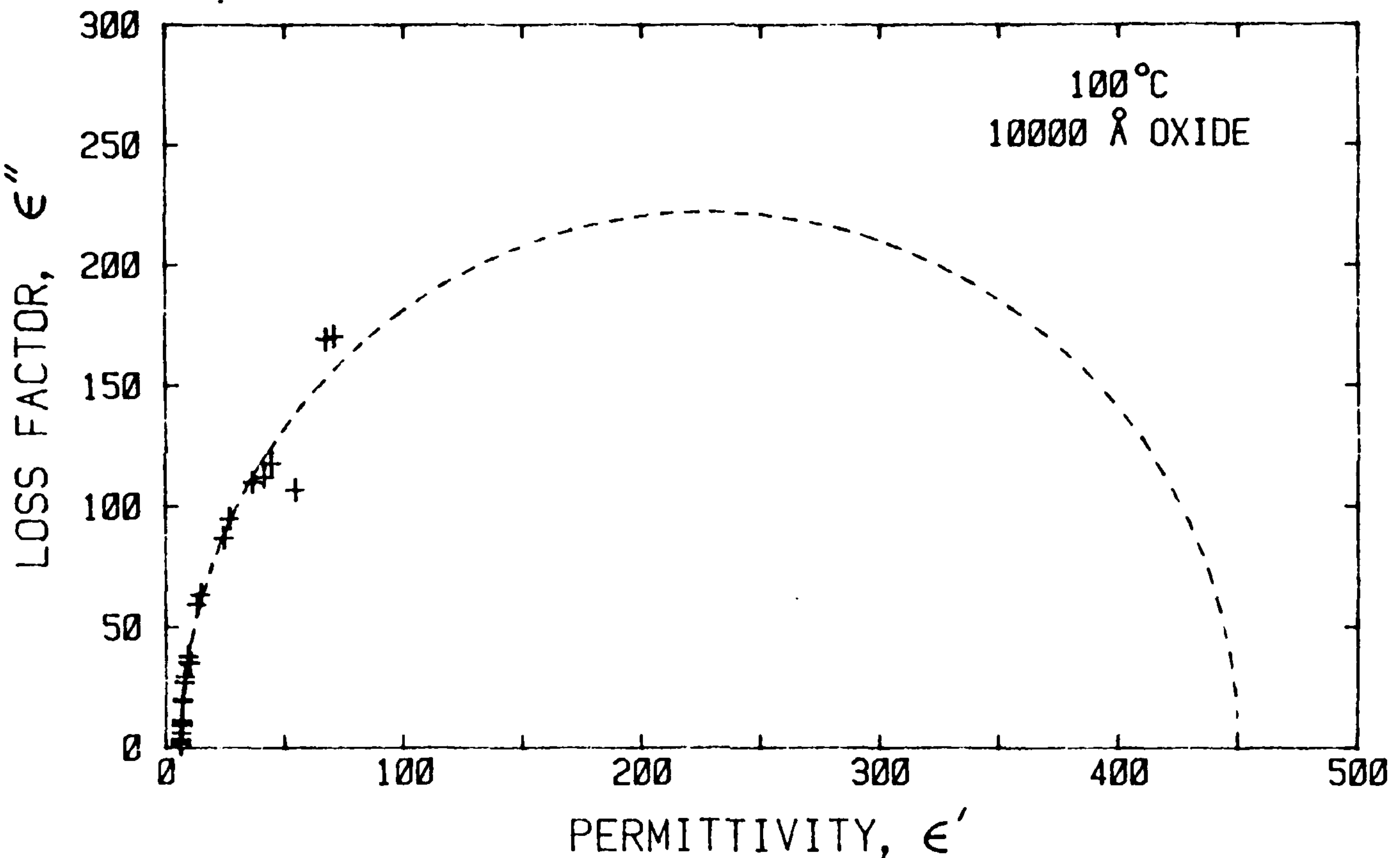

Fig. 10 Cole-Cole plot for data of Fig. 8 before gelation. Dashed line represents Debye model fit.

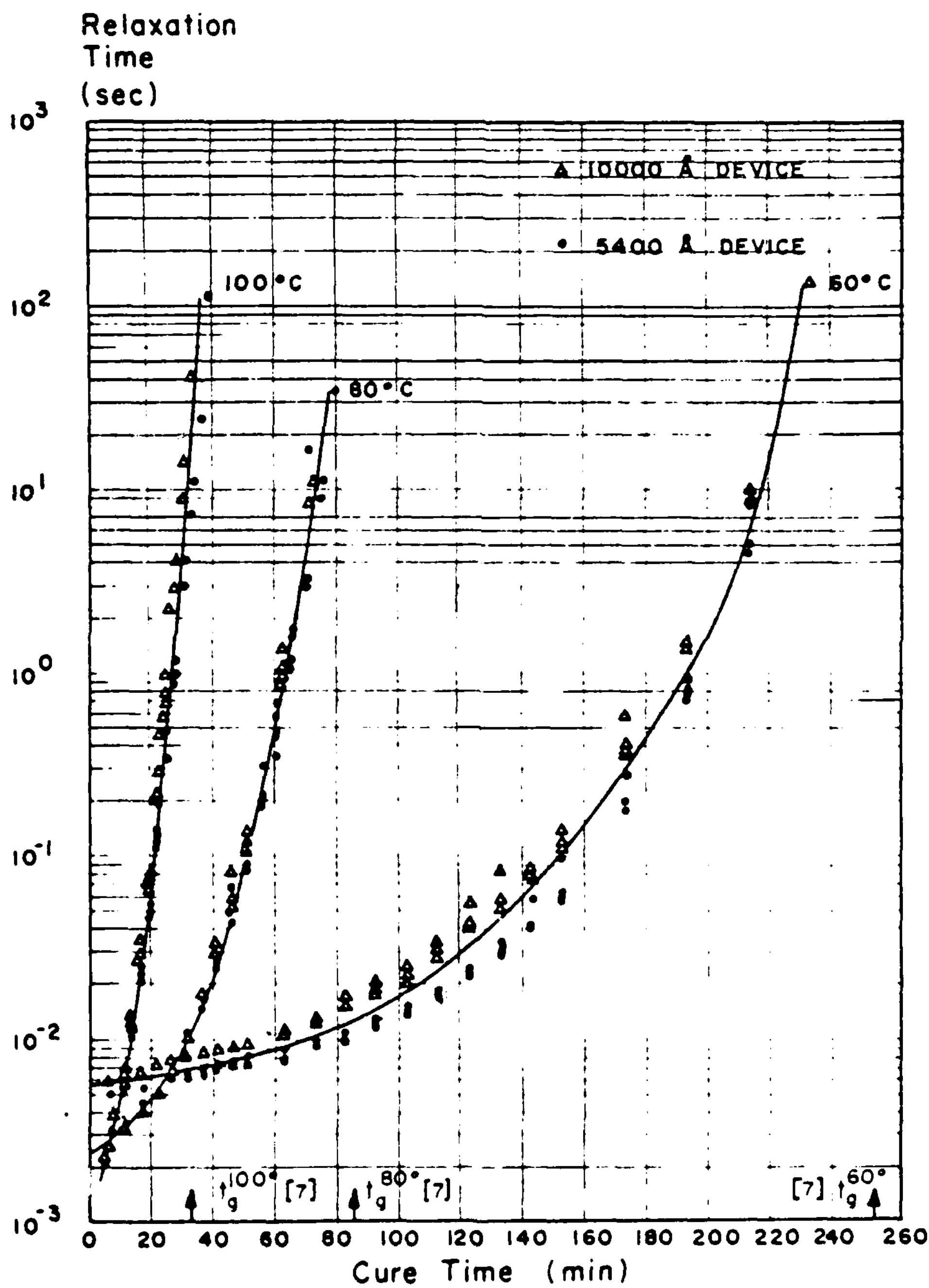

Fig. 11 Relaxation time versus cure time for all experiments

frequencies at the same elapsed cure time was within 20%. The agreement between the relaxation times determined from the devices with different oxide thicknesses at the same cure temperature was within 50%.

The time dependence of the relaxation time resembles the time dependence of the viscosity of thermosetting systems. The slope of a plot of log viscosity versus time breaks to a much steeper slope as cure proceeds, and is attributed to chain entanglement among the branched polymers formed early in cure (9). Another important similarity to viscosity is that the relaxation time at the start of cure increases as the temperature decreases. In fact, we have found an excellent correspondence between the time dependence of the relaxation time, as determined in our experiments, and the viscosity data reported by Kamal (10), by simply scaling the relaxation time axis appropriately (see Fig. 12). (A similar scaling of dielectric relaxation time and viscosity has been reported by Denney in a very different chemical system (11).) The viscosity data and relaxation time data for various temperatures form a smooth progression. As confirmation of the correspondence between the two, we have plotted in Fig. 13 an Arrhenius plot for the time to reach 400 poise or 8 seconds relaxation time. The points fall on one straight line characterized by an activation energy of 11.5 kCal/mole, indicating that the same process is responsible for the behavior of both the viscosity and the dielectric relaxation time.

VI. DISCUSSION

The results of this paper have been presented in fairly condensed form, and have been organized to emphasize the measurement technique, and the kinds of data that can be obtained with it. Clearly, there is more work to be done on device design, device packaging, and device calibration, particularly near the gain-phase origin. Nevertheless, we have found that it is possible to extract from low frequency dielectric data a quantity (the low-frequency dielectric relaxation time) which appears to carry the same information as bulk viscosity. This relaxation time can be measured entirely electrically, and the data-processing needed to convert gain-phase data to relaxation time is modest enough to be performable on a real-time basis. Thus, one can anticipate being able to monitor the viscosity of a curing system, in situ, and in real time. Given the role played by the viscosity in the determination and control of cure cycles for composites, the microdielectrometer should prove an advantageous addition to the family of cure monitoring methods.

VII. ACKNOWLEDGEMENTS

This work was supported in part by the Office of Naval Research. Particular thanks is due Dr. Leighton H. Peebles, Jr., of ONR, who originally suggested that our work on MOS sensing devices might be usefully applied to cure monitoring problems. Device fabrication was carried out in the M.I.T. Microelectronic Laboratory, a Central Facility of the Center for Materials Science and Engineering which is sponsored in part by the National Science Foundation under contract DMR-78-24185. Some of the instrumentation used in

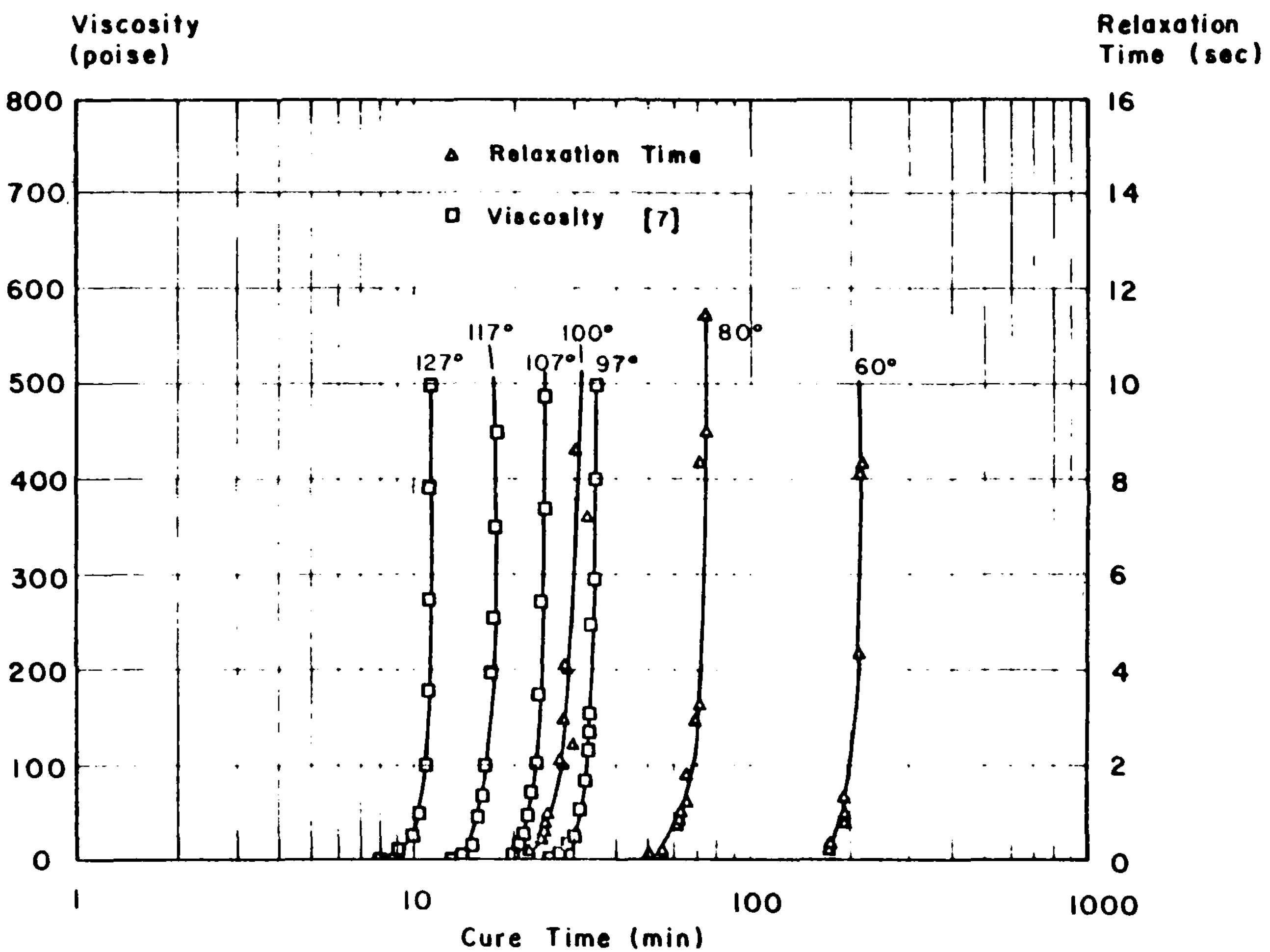

Fig. 12 Comparison between time dependences of relaxation time and viscosity.

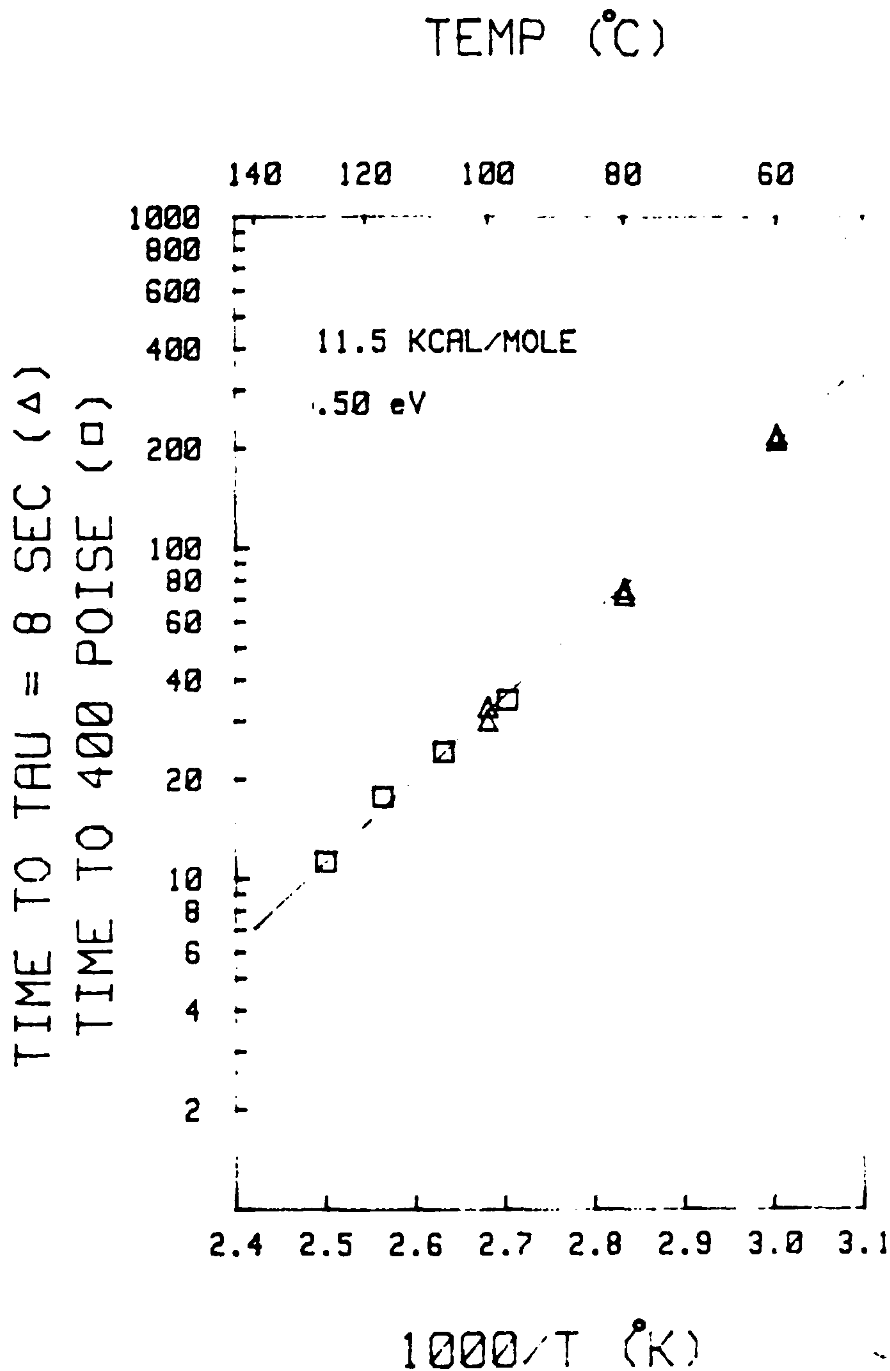

Fig. 13 Arrhenius plot of time in minutes to reach either a fixed relaxation time or a fixed viscosity.

the microdielectrometry system was purchased under NSF contract ENG-7717219. Resin samples used in these experiments were obtained from Dr. N. Schneider of the Army Materials and Mechanics Research Center.

REFERENCES

1. Norman F. Sheppard, Steven L. Garverick, David R. Day, and Stephen D. Senturia, "Microdielectrometry: A New Method for In Situ Cure Monitoring", Proc. 26th SAMPE Symposium, Los Angeles, April, 1981.

2. P. Hedvig, Dielectric Spectroscopy of Polymers, Wiley, New York, 1977.

3. S. Yalof, "Probing Structure with Dielectric Spectroscopy", Chemtech, March 1975, pp. 165-71.

4. Steven L. Garverick and Stephen D. Senturia, "An MOS Device for Surface Impedance Measurement and Moisture Monitoring", IEDM Technical Digest, pp. 685-8 (1980).

5. Huan L. Lee, S.M. Thesis, Massachusetts Institute of Technology, 1981.

6. Norman F. Sheppard, S.M. Thesis, Massachusetts Institute of Technology, 1981.

7. S. Sourour and M. R. Kamal, "Differential Scanning Calorimetry of Epoxy Cure: Isothermal Cure Kinetics", Thermochimica Acta 14, 41 (1976).

8. K. S. Cole and R. H. Cole, "Dispersion and Absorption in Dielectics", J. Chem. Phys. 9, 341 (1941).

9. F.G. Musatti and C. W. Macosko, "Rheology of Network Forming Systems", Polymer Eng. Sci. 13, 236 (1973).

10. M. R. Kamal, S. Sourour, and M. Ryan, "Integrated Thermo-rheological Analysis of the Cure of Thermosets", Technical Papers, 31st Annual Technical Conference, Society of Plastics Engineers, Montreal, May 1973, p. 187.

11. D. J. Denney, "Viscosities of Some Undercooled Liquid Alkyl Halides", J. Chem. Phys. 30, 159 (1959); "Dielectric Properties of Some Liquid Alkyl Halides", J. Chem. Phys. 27, 259 (1957).

TECHNICAL REPORT DISTRIBUTION LIST, GEN

	No. Copies
Office of Naval Research Attn: Code 472 800 North Quincy Street Arlington, Virginia 22217	2
ONR Branch Office Attn: Dr. George Sandoz 536 S. Clark Street Chicago, Illinois 60605	1
ONR Area Office Attn: Scientific Dept. 715 Broadway New York, New York 10003	1
ONR Western Regional Office 1030 East Green Street Pasadena, California 91106	1
ONR Eastern/Central Regional Office Attn: Dr. L. H. Peebles Building 114, Section D 666 Summer Street Boston, Massachusetts 02210	1
Director, Naval Research Laboratory Attn: Code 6100 Washington, D.C. 20390	1
The Assistant Secretary of the Navy (RE&S) Department of the Navy Room 4E736, Pentagon Washington, D.C. 20350	1
Commander, Naval Air Systems Command Attn: Code 310C (H. Rosenwasser) Department of the Navy Washington, D.C. 20360	1
Defense Technical Information Center Building 5, Cameron Station Alexandria, Virginia 22314	12
Dr. Fred Saalfeld Chemistry Division, Code 6100 Naval Research Laboratory Washington, D.C. 20375	1
U.S. Army Research Office Attn: CRD-AA-IP P.O. Box 1211 Research Triangle Park, N.C. 27709	1
Naval Ocean Systems Center Attn: Mr. Joe McCartney San Diego, California 92152	1
Naval Weapons Center Attn: Dr. A. B. Amster, Chemistry Division China Lake, California 93555	1
Naval Civil Engineering Laboratory Attn: Dr. R. W. Drisko Port Hueneme, California 93401	1
Department of Physics & Chemistry Naval Postgraduate School Monterey, California 93940	1
Dr. A. L. Slafkosky Scientific Advisor Commandant of the Marine Corps (Code RD-1) Washington, D.C. 20380	1
Office of Naval Research Attn: Dr. Richard S. Miller 800 N. Quincy Street Arlington, Virginia 22217	1
Naval Ship Research and Development Center Attn: Dr. G. Bosmajian, Applied Chemistry Division Annapolis, Maryland 21401	1
Naval Ocean Systems Center Attn: Dr. S. Yamamoto, Marine Sciences Division San Diego, California 91232	1
Mr. John Boyle Materials Branch Naval Ship Engineering Center Philadelphia, Pennsylvania 19112	1

SP472-3/A3

472:GAN:716:ddc
78u472-608

TECHNICAL REPORT DISTRIBUTION LIST, GEN

	No. Copies
Dr. Rudolph J. Marcus Office of Naval Research Scientific Liaison Group American Embassy APO San Francisco 96503	1
Mr. James Kelley DTNSRDC Code 2803 Annapolis, Maryland 21402	1
Dr. Henry Wohltjen Naval Research Laboratory Code 6170 Washington, DC 20390	1
Dr. Ron Trabocco Code 60631 Naval Air Development Center Warminster PA 18974	1

SP472-3/B5

472:GAN:716:ddc
78u472-608

TECHNICAL REPORT DISTRIBUTION LIST, 356A

	No. Copies
Dr. Stephen H. Carr Department of Materials Science Northwestern University Evanston, Illinois 60201	1
Dr. M. Broadhurst Bulk Properties Section National Bureau of Standards U.S. Department of Commerce Washington, D.C. 20234	2
Professor G. Whitesides Department of Chemistry Massachusetts Institute of Technology Cambridge, Massachusetts 02139	1
Professor J. Wang Department of Chemistry University of Utah Salt Lake City, Utah 84112	1
Dr. V. Stannett Department of Chemical Engineering North Carolina State University Raleigh, North Carolina 27607	1
Dr. D. R. Uhlmann Department of Metallurgy and Material Science Massachusetts Institute of Technology Cambridge, Massachusetts 02139	1
Naval Surface Weapons Center Attn: Dr. J. M. Augl, Dr. B. Hartman White Oak Silver Spring, Maryland 20910	1
Dr. G. Goodman Globe Union Incorporated 5757 North Green Bay Avenue Milwaukee, Wisconsin 53201	1
Professor Hatsuo Ishida Department of Macromolecular Science Case-Western Reserve University Cleveland, Ohio 44106	1
Picatinny Arsenal Attn: A. M. Anzalone, Building 3401 SMUPA-FR-M-D Dover, New Jersey 07801	1
Dr. J. K. Gillham Department of Chemistry Princeton University Princeton, New Jersey 08540	1
Douglas Aircraft Co. Attn: Technical Library C1 290/36-84 AUTO-Sutton 3855 Lakewood Boulevard Long Beach, California 90846	1
Dr. E. Baer Department of Macromolecular Science Case Western Reserve University Cleveland, Ohio 44106	1
Dr. K. D. Pae Department of Mechanics and Materials Science Rutgers University New Brunswick, New Jersey 08903	1
NASA-Lewis Research Center Attn: Dr. T. T. Serofini, MS-49-1 21000 Brookpark Road Cleveland, Ohio 44135	1
Dr. Charles H. Sherman Code TD 121 Naval Underwater Systems Center New London, Connecticut	1
Dr. William Risen Department of Chemistry Brown University Providence, Rhode Island 02192	1
Dr. Alan Gent Department of Physics University of Akron Akron, Ohio 44304	1

TECHNICAL REPORT DISTRIBUTION LIST, 356A

	No. Copies
Mr. Robert W. Jones Advanced Projects Manager Hughes Aircraft Company Mail Station D 132 Culver City, California 90230	1
Dr. C. Giori IIT Research Institute 10 West 35 Street Chicago, Illinois 60616	1
Dr. M. Litt Department of Macromolecular Science Case Western Reserve University Cleveland, Ohio 44106	1
Dr. R. S. Roe Department of of Materials Science and Metallurgical Engineering University of Cincinnati Cincinnati, Ohio 45221	1
Dr. Robert E. Cohen Chemical Engineering Department Massachusetts Institute of Technology Cambridge, Massachusetts 02139	1
Dr. T. P. Conlon, Jr., Code 3622 Sandia Laboratories Sandia Corporation Albuquerque, New Mexico	1
Dr. Martin Kaufmann, Head Materials Research Branch, Code 4542 Naval Weapons Center China Lake, California 93555	1
Dr. T. J. Reinhart, Jr., Chief Composite and Fibrous Materials Branch Nonmetallic Materials Division Department of the Air Force Air Force Materials Laboratory (AFSC) Wright-Patterson AFB, Ohio 45433	1
Dr. J. Lando Department of Macromolecular Science Case Western Reserve University Cleveland, Ohio 44106	1
Dr. J. White Chemical and Metallurgical Engineering University of Tennessee Knoxville, Tennessee 37916	1
Dr. J. A. Manson Materials Research Center Lehigh University Bethlehem, Pennsylvania 18015	1
Dr. R. F. Helmreich Contract RD&E Dow Chemical Co. Midland, Michigan 48640	1
Dr. R. S. Porter Department of Polymer Science and Engineering University of Massachusetts Amherst, Massachusetts 01002	1
Professor Garth Wilkes Department of Chemical Engineering Virginia Polytechnic Institute and State University Blacksburg, Virginia 24061	1
Dr. Kurt Baum Fluorochem Inc. 6233 North Irwindale Avenue Azuza, California 91702	1
Professor C. S. Paik Sung Department of Materials Sciences and Engineering Room 8-109 Massachusetts Institute of Technology Cambridge, Massachusetts 02139	1

DAT
FILM